ORIGINAL PAPER

A strategy for visual optical determination of glucose based on a smartphone device using fluorescent boron-doped carbon nanoparticles as a light-up probe

Negar Alizadeh[1] · Abdollah Salimi[1,2] · Rahman Hallaj[1,3]

Abstract

Boronic acid-doped carbon nanoparticles were prepared and are shown to undergo aggregation induced emission (AIE). The nanoparticle composite is a viable fluorescent probe for glucose determination by using the RGB technique and a smartphone. The structure and the chemical composition of the doped carbon nanoparticles were confirmed by SEM, TEM, FTIR and UV-vis spectroscopy. The combination of 4-carboxyphenylboronic acid with o-phenylenediamine and rhodamine B endowed the hybrid with high fluorescence intensity (quantum yield 46%). Compared with conventional two-step preparation of boronic acid-based fluorescent probes for glucose, the present one step synthesis strategy is simpler and more effective. The addition of glucose causes the formation of covalent bonds between the cis-diols group of glucose molecules and boronic acid moiety. Fluorescent intensity can be quantified using dual wavelengths simultaneously, where both increases, as the target analytes bind to the bronic acid. These variations was monitored by the smartphone camera, and the green channel intensities of the colored images were processed by using the RGB option of a smartphone. The assay works in the 32 μM to 2 mM glucose concentration range and has an 8 μM detection limit. The method was successfully used for the assay of glucose in diluted human serum.

Keywords Glucose sensing · Fluorescence · Carbon nanoparticle · Bronic acid · Point of care · Smartphone

Introduction

More than 117 million people suffer from diabetes around the world, and it was forecast that the figure will reach 300 million by 2025 [1, 2]. Reliable methods for measuring blood glucose level is essential to manage diabetes progression and treatment [3]. The most common methods for glucose monitoring are enzyme-based [4]. In these sensors, glucose oxidase (GOx) oxidizes glucose and produces hydrogen peroxide, which leads to indirectly measuring of glucose level by monitoring the redox reaction of hydrogen peroxide [5]. However, the high cost and instability of enzyme limit the application of enzyme-based glucose sensors [6]. The other method for determination of glucose is a system without the enzyme by designing and synthesizing probe for glucose [7]. Compared with the enzymatic glucose sensor, the non-enzymatic system offers several advantages such as higher stability, lower cost, and easier preparation [8].

The diol compounds and boronic acid has been applied as a chemical receptors and molecular recognition tool instead of GOx bio-receptors in non-enzymatic glucose sensor [9]. Boronic acid has a high affinity to reaction with compounds containing 1,2-diols or 1,3-diols through a reversible ester formation [10]. Various detection methods such as electrochemical [11], surface enhanced raman spectroscopy (SERS) [12], colorimetric [13] and fluorescence [14] was developed based on boronate

✉ Abdollah Salimi
absalimi@uok.ac.ir; absalimi@yahoo.com

1   Department of Chemistry, University of Kurdistan, Sanandaj 66177-15175, Iran

2   Department of Chemistry, University of Western Ontario, London, Ontario N6A 5B7, Canada

3   Research Center for Nanotechnology, University of Kurdistan, Sanandaj 66177-15175, Iran

affinity for non-enzymatic glucose detection. Among various measuring method, fluorescence detection is more attractive because provides advantages of high sensitivity, simplicity of operation and non-invasiveness [15]. In this regard, it is important to develop an accurate non-enzymatic fluorescent strategy as alternative for the detection of glucose. For instance, Naaz et al. designed fluorescent silver nanoclusters anchored with 3-aminophenyl boronic acid (AgNCs-a-APBA) for precise determination of blood glucose level [16]. In this strategy, the hydrogen bonding-driven aggregation of APBA with AgNCs enhance the fluorescence intensity of AgNCs. Upon addition of glucose, disaggregation of the nanoclusters triggered and photoluminescence (PL) intensity decreased. Most of fluorescent platform for nonenzymatic glucose sensing is based on the two-step fabrication of nanoparticle [9]. However, we designed bronic acid fluorescence probe through one step hydrothermal process.

Portable analytical platform has offered on-the-spot sample detection as a potential alternative to conventional analytical methodologies. These new methodologies are specially designed to provide analytical information in a simple, inexpensive and rapid way for in-situ analysis [17]. With the increase in the widespread smartphone popularity, mobile point-of-care technology (MPOCT) has shown promise in meeting the needs of decentralized laboratory testing [18]. Pocket-size smartphones as a handheld device camera enables image acquisition with the high-resolution. The images acquired using this smartphone can be used for quantification of target analytes based on the characteristics such as color and overall fluorescence intensity [19].

In this study, we describe a smartphone based method with low cost and high portability to detect glucose in blood serum sample. We synthesized carbon nanoparticle containing of boric acid as a new fluorescent receptor for glucose assay applications. The carbon nanoparticles are directly functionalized by boronic acids (binding sites) in the one step, without need to additional surface modification. The glucose selectively lead to the aggregation of the BCNP peobe based on the covalent binding between the cis-diols of glucose and boronic acid [20], resulting in a linear fluorescence increase in the range of 0.032–2 mM with detection limit of 8 μM. The overall work is illustrated in Scheme 1, which depicts the applications of the as synthesized BCNP probe for glucose detection using smartphone based platform. Besides, the designed fluorescent nanoprobe was applied for quantitative detection of glucose in the serum sample. Thus, it has great promise as a facile practical platform for clinical glucose sensing.

Experimental

Materials and instruments

4-Carboxyphenylboronic acid (4-CPBA), o-phenylenediamine (OPD) and rhodamine B (Rh B), glucose, ascorbic acid (AA), dopamine (DA), uric acid (UA), glucose, L-glutathione (GSH), KCl, NaCl, CaCl$_2$, MgCl$_2$, alanine (Ala), arginine (Ag), cysteine (Cys), homocysteine (H-Cys), tryptophan (Thr), proline (Pro) and serine (Ser) were purchased from Sigma Aldrich (United States, http://www.sigma-aldrich.com/). All the reagents were used without any further purification. Deionized water from a Milli-Q Plus system (Millipore) was used in all solutions and experiment.

The fluorescence spectra and the UV-Vis absorption spectra were measured at room temperature on a spectrophotometer Varian Cary Eclipse Fluorescence Spectrophotometer and a SPECTROD 250-analytikjena spectrophotometer, respectively. The morphology of product was characterized by scanning electron microscope (SEM) on a MIRA3 TESCAN HV: 20.0 KV from Czech Republic, transmission electron microscope (TEM) and the Fourier transform infrared (FTIR) spectrum was recorded on a Vector-22 BRUKER spectrophotometer (Switzerland). All images were acquired using the HTC (ONE SV) from Apple (unless otherwise specified) mounted in designed device.

Synthesis of fluorescent BCNP

The carbon nanoparticles prepared from phenylbronic acid, rhodamine B and OPD as the monomer. In a typical procedure, 14 mg OPD was dissolved in 10 mL NaOH (0.05 M) and stirred for 30 min. Afterward, 10 mL of 4-carboxyphenylboronic acid (0.08 mM) was added to above solution with continuous stirring for 2 h at room temperature. Then, 5 mL of rhodamine B was poured into the solution. After 30 min stirring, the mixture was transferred to the 50 mL Teflon-lined stainless-steel autoclave and heated hydrothermally at 150 °C for 5 h. After cooled down to room temperature, the product was centrifuged, and the residual precipitate was removed and then the supernatant was kept at 4 °C for further use.

Quantum yields

The quantum yield (Q) of BCNP was determined by using fluorescein in 0.1 M NaOH as the standard sample and calculated according to the following equation:

$$Q = Q_R*(Grad/Grad_R)*(n^2/n^2_R)$$

Where Q is the quantum yield, Grad is gradient from the plot of integrated fluorescence intensity vs absorbance, n is the
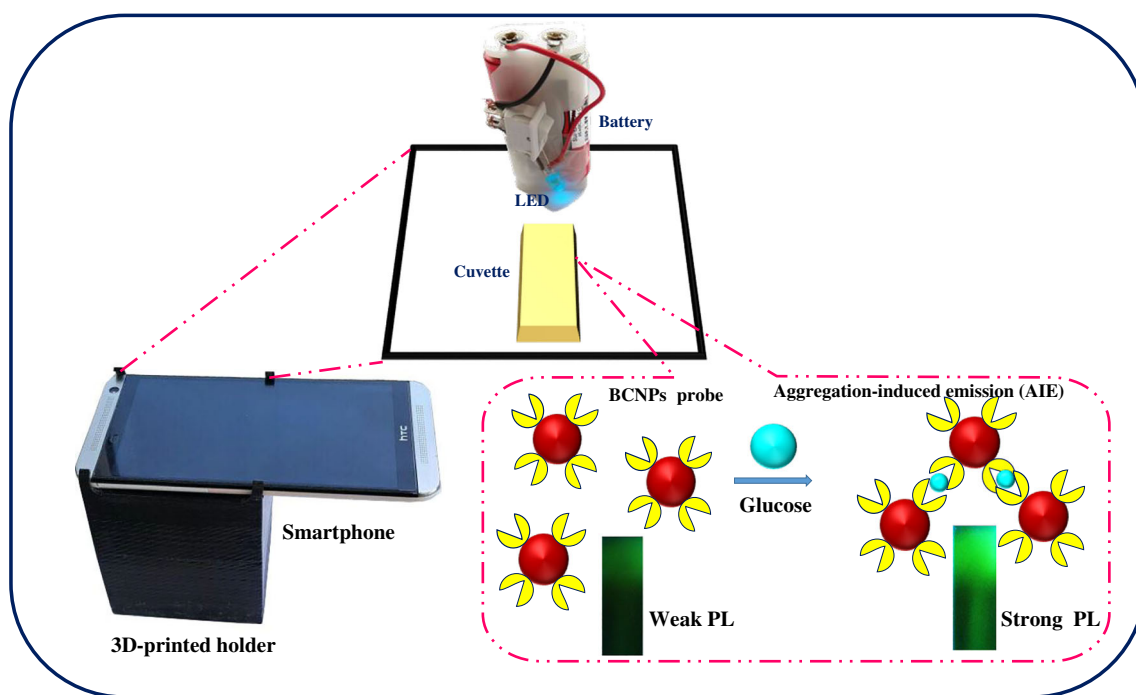
Scheme 1 Schematic illustration of fluorometric determination of glucose based on Aggregation-Induced Emission (AIE)

refractive index of the solvent (1.33 for water). The subscript *R* refers to the reference with a known quantum yield.

Procedures for glucose sensing

The mobile phone-based system for luminescence measurements was designed using rhinoceros 5 and 3D printed commercially (3d print industrial fdm ZBOT i2s). The custom designed device is comprised of a 3D-printed holder containing an LED as a light source, two electric batteries as a power source and a button cell for keeping the sample solution. The blue LED was selected as the light source to quantify the glucose level. 300 μL of BCNP were placed in a series of microtubes. Then, different concentration of glucose was added. The mixtures were transferred to quartz fluorescent cuvette. Then fluorescence spectra and images were recorded. The image analysis was performed through RGB analysis software installed on smartphone. As the concentration of glucose increased the PL intensity of both peak at 450 and 550 increased. As well as, the variation in brightness corresponds to increasing concentrations of glucose. Same procedure was followed for plasma serum samples.

Selectivity of BCNP to glucose determination

GSH, DA, UA, K^+, Na^+, Mg^{2+}, Ca^{2+}, Ala, Ag, Cys, H-Cys, Thr, Pro and Ser were selected to evaluate the selectivity of BCNP toward glucose sensing. Each of BCNP solutions in 1.5 mL tubes, containing various interference were incubated for 2 h at room temperature, and their fluorescence responses were measured. The responses to glucose and the interference on BCNP were compared.

## Determination of glucose in serum samples

The fresh human serum samples with different concentration of glucose were collected from the local hospital. All the blood samples were obtained through venipuncture and necessary processes were accomplished to remove large molecules and proteins to get the serum samples. The original serum samples were diluted in order to guarantee the glucose content in samples was in the range of our established standard curve. 10 μL of the serum samples was added to 300 μL of stock solution of BCNP probe. After 30 min, the fluorescence images were recorded under excitation of blue LED lamp using smartphone. The obtained results were compared with clinical laboratory analysis as the standard method using local hospital-used instrument (Biotecnica BT 4500).

Results and discussion

Characterizations of BCNP

The BCNP was synthesized by a one step and facile hydrothermal method. The morphology and size of BCNP was characterized by taking of SEM and TEM images (Fig. 1a, b). It shows that BCNP are spherical with an average size of about 30 nm. The molecular structure of OPD, 4-CPBA and BCNP was also investigated by FT-IR spectra.

Fig. 1 (**A**, **B**) SEM and TEM images of BCNP, (**C**) FTIR spectrum of (**a**) OPD, (**b**) 4-CPBA, (**c**) Rh B, (**d**) BCNP
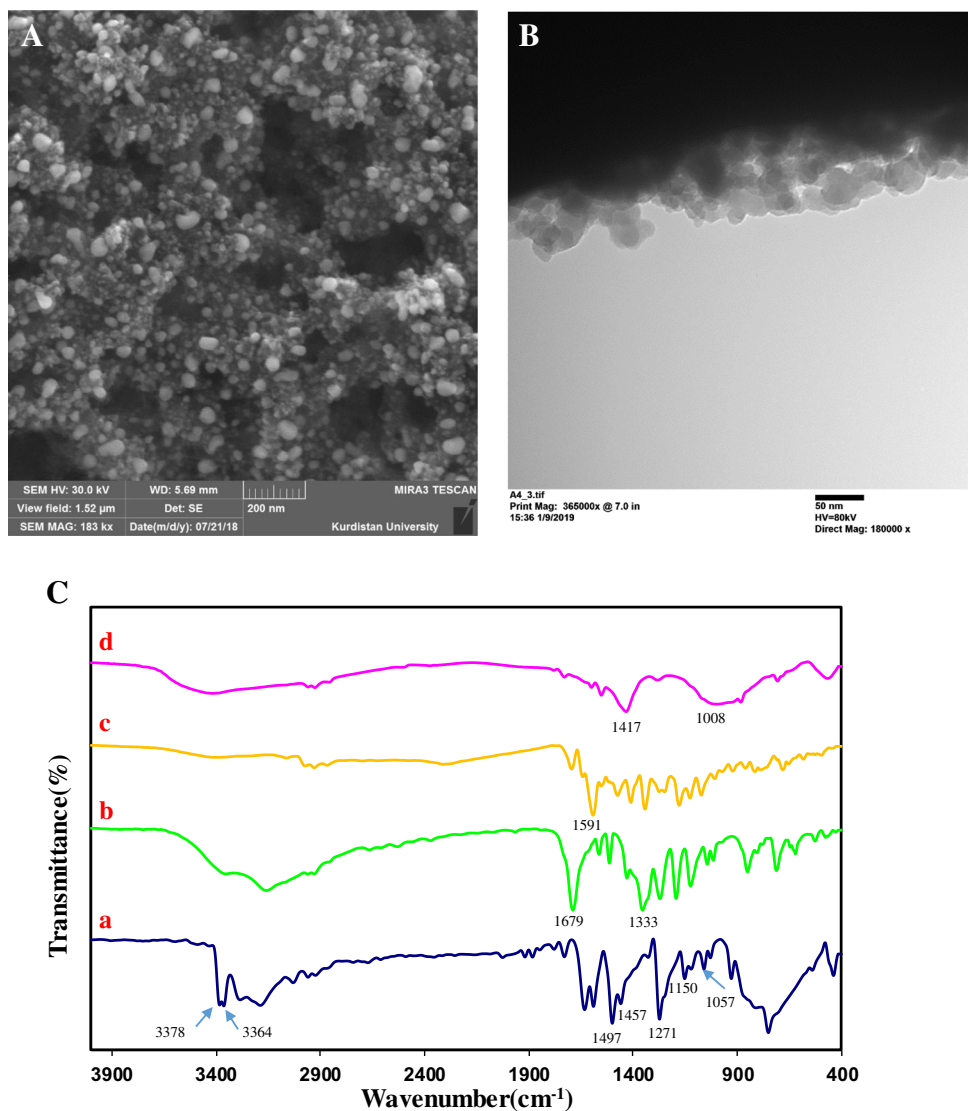

As shown in Fig. 1c, the peaks at 3378 cm^{-1} and 3364 cm^{-1} in the spectrum of OPD can be assigned to asymmetrical and symmetrical N–H stretching vibrations. The two peaks at 1457 cm^{-1} and 1497 cm^{-1} are the characteristic bands of the C=C stretching vibrations for benzenoid rings, while the peaks at 1057 cm^{-1}, 1150 cm^{-1} and 1271 cm^{-1} are due to C–N stretching vibrations (curve a) [21]. In the FT-IR spectrum of 4-CPBA the broad absorption band in the range of 3000 and 3300 cm^{-1} and the peak at 1679 cm^{-1} was attributed to O–H and C=O stretching of carboxylic acid group, respectively. The absorption band in 1600–1400 cm^{-1} region was assigned to C=C framework vibration of benzene ring; the peak at 1333 cm^{-1} is due to the B–O stretching vibration of boroxol bond in the 4-CPBA. Also, the band in the 1300–1000 cm^{-1} region was attributed to C–O stretching of alkoxy bond (curve b) [22]. The peak at 1591 cm^{-1} is assigned to C=O carboxyl group from the rhodamine B molecule (curve c) [23]. The IR

spectrum of synthesized BCNP is different from the monomers, in which a new absorption at 1417 cm^{-1} was observed corresponding to the stretching vibration of C–N amide group and the broad peak at 1008 cm^{-1} is related to the C–B stretching vibration (curve d). Furthermore, the disappearance or decrease of other absorption peaks mean that the carbon was formed successfully.

The XPS measurement was conducted to investigate the elemental composition and chemical bonding state. The XPS survey spectrum of BCNP comprises the peaks corresponding to carbon (59.6.5%), oxygen (24.8%), nitrogen (1.0%) and boron (0.4%) elements (Fig. 2a). The high resolution spectrum of B 1 s demonstrated two peaks with binding energies of 192.07 and 192.77 eV, corresponding to B–C and B–O (Fig. 2b) [24]. The high resolution C 1 s spectrum (Fig. 2c) shows the presence of carboxylic groups at 288.17 as well as C–O/C–N and C=C bonds at 285.27 and 284.47, respectively. The

Fig. 2 XPS spectrum of boron-doped CNPs: (**a**) survey XPS spectrum with atomic content. (**b**) High-resolution B 1 s spectrum. (**c**) High-resolution C 1 s spectrum. (**d**) High resolution N 1 s spectrum
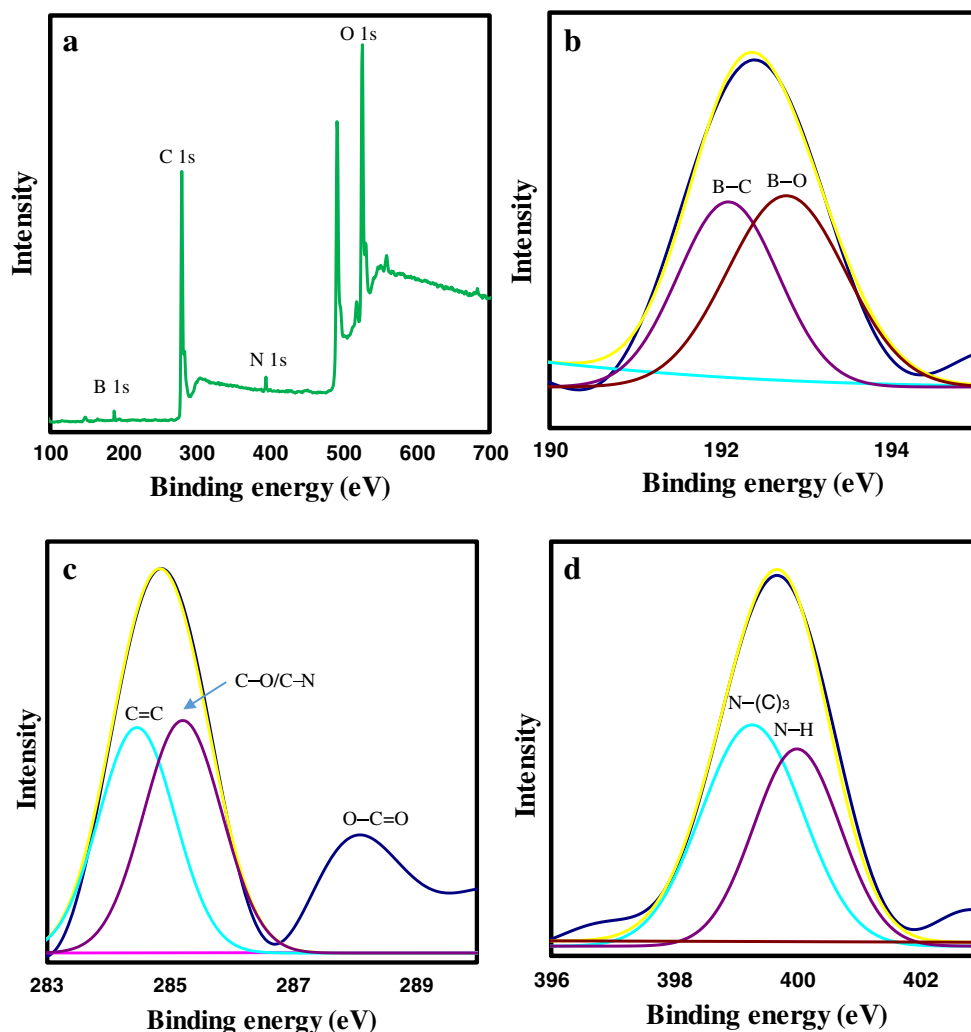
N 1 s spectrum shows two obvious peaks at 399.27 and 400.07 eV, giving two components for N–(C)$_3$ and N–H (Fig. 2d) [25].

The optical properties of BCNP

As shown in the UV-Vis spectrum in Fig. 3a, the BCNP show the obvious absorption bands at 427 nm. While, the absorption spectrum of RhB features a typical band at 554 nm characteristic to the S0-S1 transitions in the xanthene ring [26] (Fig. 3b). In comparison to RhB organic dye the absorption spectrum of BCNP was broader and exhibited the 127 nm blue shift, that is, from $\lambda = 554$ to 427 nm. As well as, Fig. 3b displays the recorded PL spectra of RhB and BCNP under the same excitation. Furthermore, as illustrated about 7 nm blue shift (from $\lambda = 580$ to 573 nm) have observed in the PL spectrum of BCNP compared to the RhB alone. This is another evidence of the successful formation of the carbon nanoparticle. The BCNP solution was bright orange under visible light, but exhibits bright yellow luminescence under blue LED lamp irradiation (the inset in Fig. 3a). Figure 3a shows the PL emission spectra of the BCNP with different excitation wavelengths from 370 to 450 nm. It can be seen that the PL emission wavelength firstly red-shift with varying excitation wavelengths from 370 to 410 nm and then blue-shift from 430 to 450 nm, which indicates the excitation-dependent fluorescence behavior of BCNP. The effect of pH on fluorescence response of the nanocomposite was investigated. As shown in Fig. 3c, the fluorescence intensities of BCNP remained nearly constant at a pH range of 6–12.

Analytical performance of nanoprobe for detection of glucose

Prior to the evaluation of the assay sensitivity, the effect of reaction time between glucose and BCNP probe on the fluorescence response of the nanoprobe was investigated. In the presence of 0.05 mM glucose, the fluorescence intensities, I_{540} and I_{640}, increased with increasing of reaction time and then reached constant when the reaction time was up to 30 min, indicating that it was a suitable reaction time for the fluorescence enhancing of the BCNP probe by glucose (Fig. 3d). So,
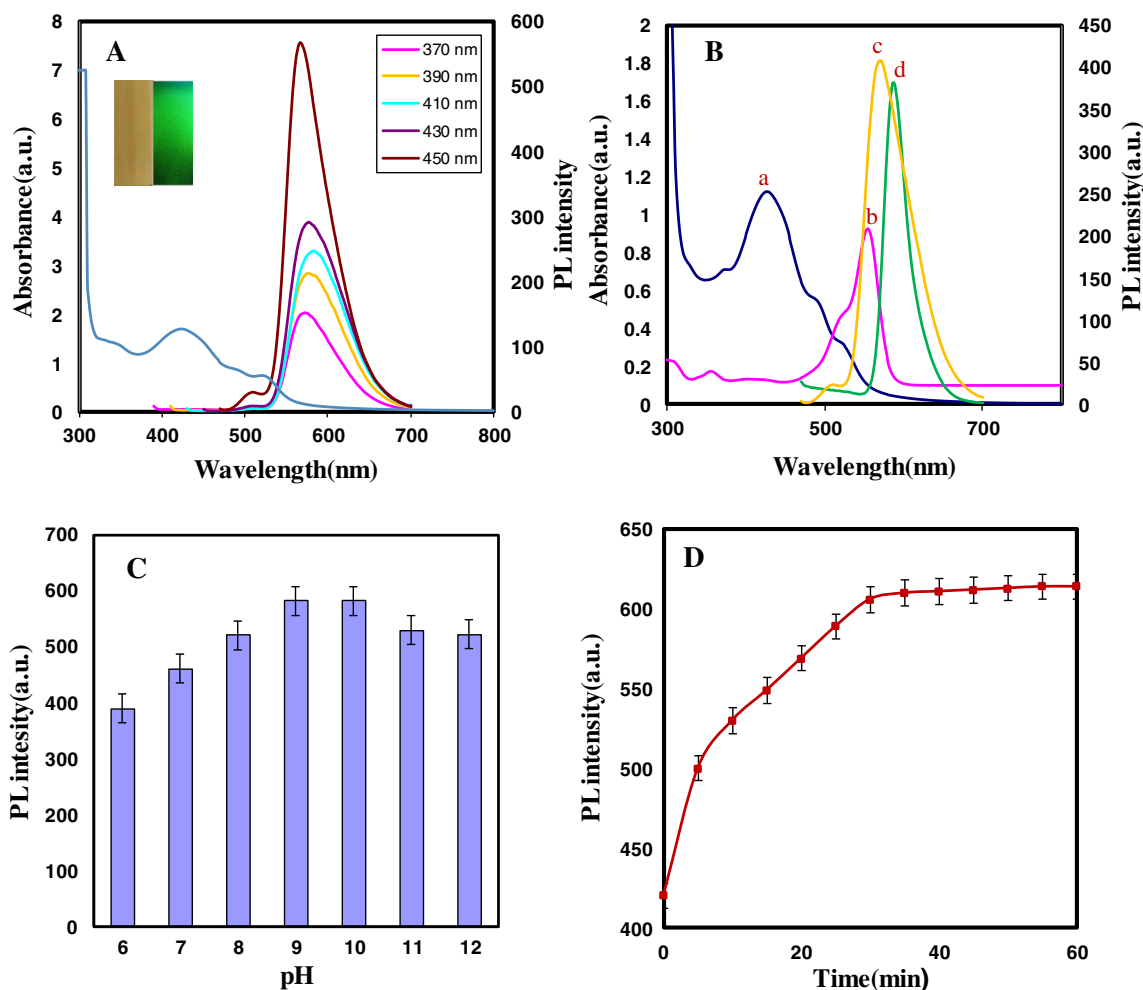
Fig. 3 (**A**) UV-vis absorption and excitation-dependent PL behavior of BCNP. (**B**) the UV-vis and PL spectra of (**a**, **c**) BCNP and (**b**, **d**) Rh B, respectively. (**C**) The influence of pH on the fluorescence intensity of BCNP at emission of 550 nm, and (**D**) Time-dependent PL intensity of BCNP upon addition of glucose

the reaction time 30 min is used as the optimized detection time throughout the following works. Figure 4b and inserted calibration plot shows the fluorescent spectra of the BCNP probe in the presence of different concentration of glucose. Upon the addition of glucose, the fluorescence intensities of the probe was gradually increased. The fluorometric signal acquired at excitation/emission wavelengths of 450/ 540,640 nm. Then, we evaluated the analytical performance of nano-based fluorescent assay under blue LED lamp irradiation after reacted with various concentration of glucose on designed smartphone based-device. As shown in Fig. 4c, the corresponding fluorescence emission increased with the increasing glucose, and a good linear correlation between green color intensity and glucose concentration was obtained within the dynamic range from 32 μM to 2 mM with a correlation coefficient (*r*) of 0.9931 (Fig. 4d). A limit of detection (LOD) of 8 μM is achieved for glucose detection, which, is much lower than the normal glucose level in human blood (3.6–6.6 mM) [27]. The analytical properties of this assay was

compared with other fluorescence based glucose sensing methods. As shown in Table 1 the detection limit and linear concentration range of the presented method is comparable or better than reported values in literature.

Selectivity and stability of BCNP probe toward glucose detection

Selectivity is a very important factor to be considered for developing and applications of detection method in biomedical samples. Accordingly, we tested the selectivity of fluorescence strategy with various interference substances. Figure 4a, presents the interference effect of some biological molecules, saccharides, common inorganic ions and amino acids including GSH, DA, UA, catechol, fructose, maltose, K^{+}, Na^{+}, Mg^{2+}, Ca^{2+}, Ala, Ag, Cys, H-Cys, Thr, Pro and Ser on the nanoprobe response. An obvious selective response was observed for glucose and no interference was found for all tested compounds at reasonable concentrations. Based on these results, our sensing strategy based

Fig. 4 (**A**) Selectivity of sensing system towards glucose and other biological relevant reactive species. Experimental conditions: 100 μM of glucose and other interference including (**a**) dopamine (DA), (**b**) glutathione (Reduced) (GSH), (**c**) AA, (**d**) urine acid (UA), (**e**) catechol (**f**) fructose (**g**) maltose (**h**) homo-cysteine, (**i**) arginine, (**j**) cysteine, (**k**) proline, (**l**) creatinine, (**m**) serine; (**n**) alanine, (**o**) L-therionine, (**p**) Hg^{2+}, (**q**) Mg^{2+}, (**r**) K^+, (**s**) Ca^{2+}, (**t**) Na^+, (**u**) glucose. (F0 and F are the fluorescence intensities of PNF in the absence and presence of ascorbic acid, respectively). (**B**) Fluorescence responses of PNF upon addition of various concentrations of glucose 0, 0.032, 0.05, 0.072, 0.162, 0.364, 0.82, and 2 mM (from 1 to 7). (**C**) Fluorescence response of the BCNP probe to various concentrations of glucose analyzed by the smartphone, and (**D**) The linear calibration plot of green color intensity versus the concentration of glucose
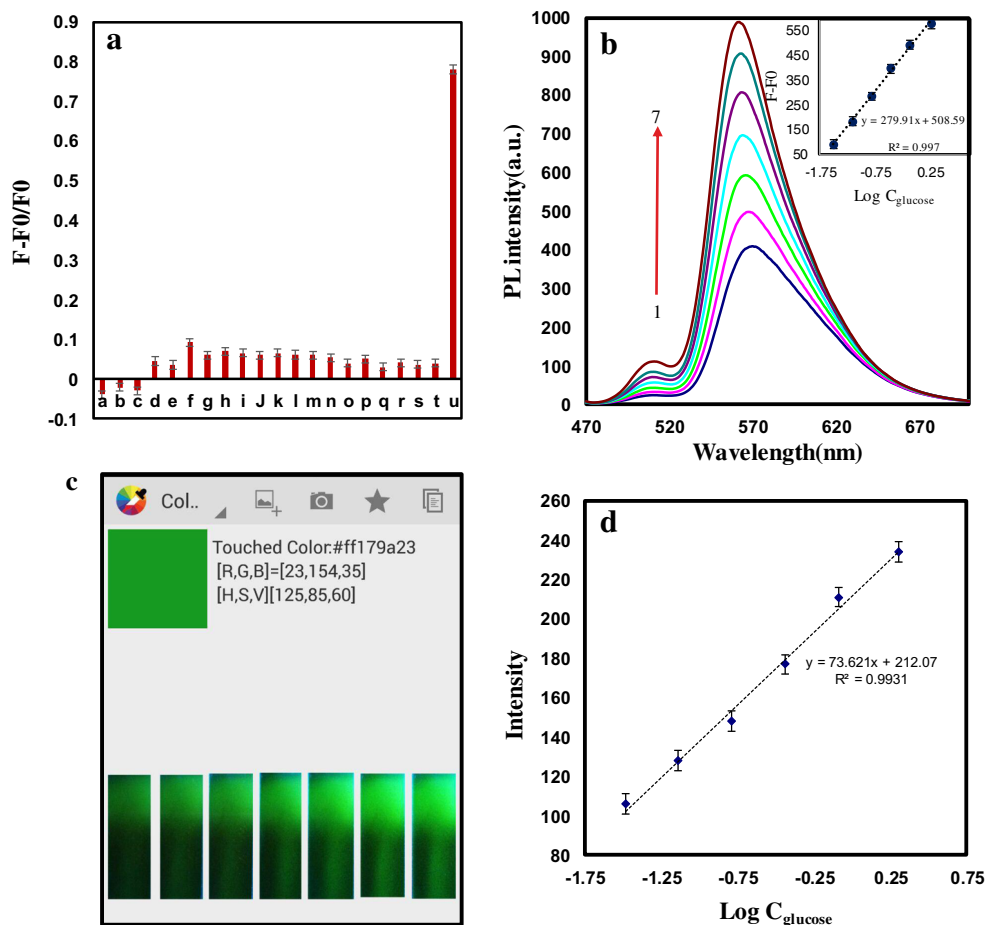
on BCNP probe can be applied as a selective assay for glucose determination without significant interference. In order to examine the stability of the glucose BCNP probe, the fluorescent spectra were checked after the probe was stored for 10, 20, and 30 days. The results indicated that 94.9% of the fluorescent intensity was maintained after 10 days, and 93.7% was maintained after a 20 days. Yet, after a month, 90.8% of the fluorescent intensity was maintained, indicating the excellent stability of the nanoprobe.

Glucose analysis in real samples

To evaluate the practical application of the sensing strategy, the detection of glucose in blood serum samples was performed. As shown in Table 2, the concentrations of glucose in human serum samples are lot of matching with the results measured by a blood sugar analyzer in hospital. As can be seen the recoveries based on our method in the real samples are between 95.00 and 102.66%, as well as, the relative

Table 1 Comparison of analytical properties of different fluorescent systems for glucose sensing

Probes	Linear range (mM)	Detection limit (μM)	Reference
CdTe/ZnTe/ZnS QDs	0.4–20	300	[28]
graphene QDs	0.1–10	5.0	[20]
CdS/polymer QDs	1–25	–	[29]
PNIPAM microgels	5–100	–	[30]
AuNCs	0.5–10	100	[31]
RGO-PBA	2–75	–	[32]
COP-1 and COP-2	0–20	600 and 2000	[33]
BCNP probe	0.032–2	8	this work

Table 2   Detection of glucose in human serum samples

| Sample	Content (mmol/L)	Found (mmol/L)	Recovery (%)	RSD ($n = 3$) (%)
1	0.05	0.048	96	3.61
2	0.15	0.154	103	4.84
3	0.25	0.256	103	2.49
4	0.50	0.475	95	3.92

standard deviations (RSD) are not higher than 4.84%. The aforementioned results confirmed applicability of the detection system for glucose sensing in biological samples.

Fluorescence sensing mechanism of the BCNP probe toward glucose detection

On the basis of the previous studies and our above experimental data, boronic acid has a high affinity to reaction with compounds containing 1,2-diols or 1,3-diols through a reversible ester formation [31]. So, the fluorescent compound containing boronic acid derivatives can construct the fluorescent probe for sensing saccharides. We employed TEM characterization to investigate fluorescent mechanism of glucose sensing. As shown in Fig. 5a, b upon interaction of BCNP with 1 mM glucose, the aggregation of BCNP was observed, suggesting aggregation-induced emission (AIE) mechanism. Since the discovery of AIE phenomenon in 2001, tetraphenylethylene (TPE) and its derivatives featuring typical AIE characteristics have been widely used to make up highly emissive fluorescent materials for optical sensing applications [34]. AIE is an abnormal phenomenon, in which, the organic luminophores with freely-rotating groups consume energy and promote radiation-less decay after excitation in solution, however, when these luminophores aggregate, the free rotation of those groups is restricted and cause to the enhancement of the photoluminescence efficiency [35]. In our study, the linkage of glucose to bronic acid moieties of BCNP, led to blocks the

Fig. 5 TEM image of the BCNP (**a**) before and (**b**) after treatment with 1 mM glucose, AFM image of the BCNP (**c**) before and (**d**) after treatment with 1 mM glucose
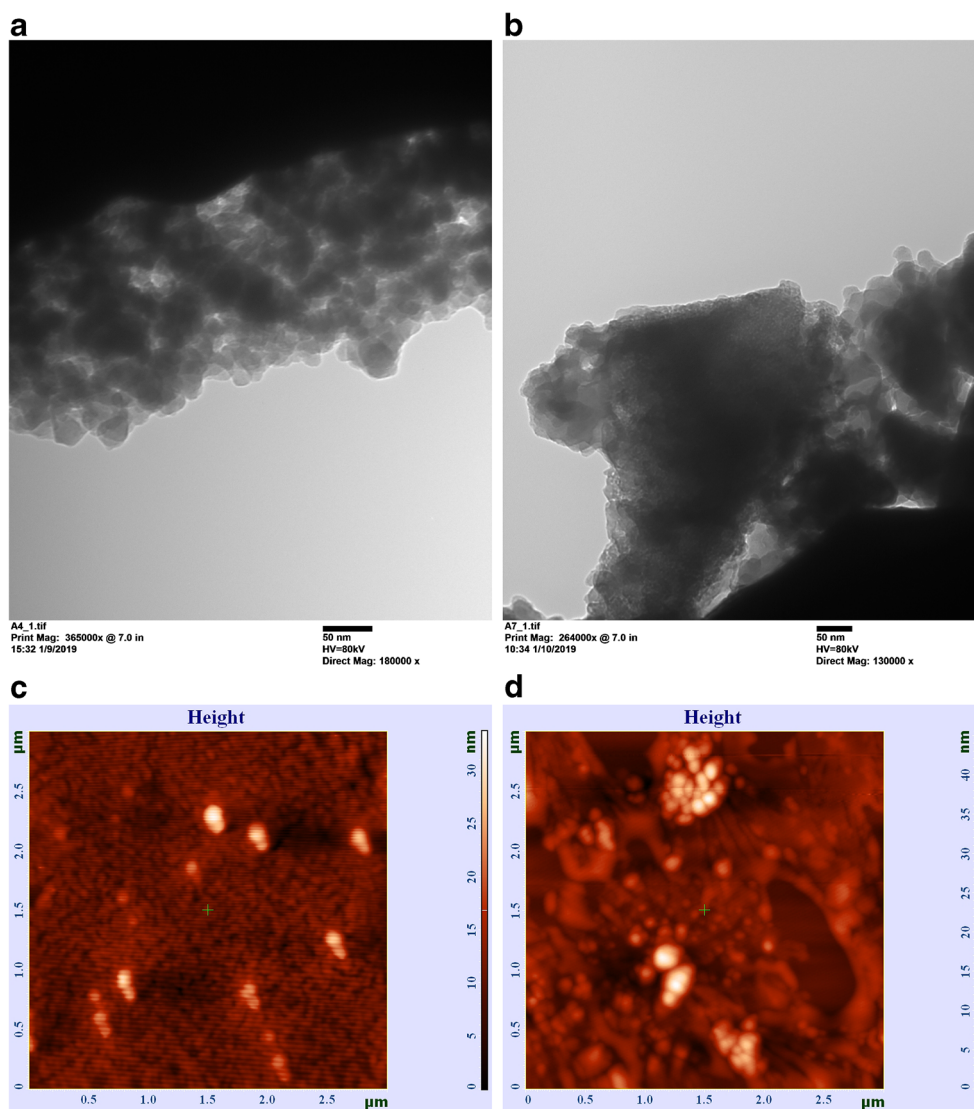
nonradiative relaxation channels and make the luminescence center highly emissive. AFM images also gave direct information on the aggregation of the BCNP, after addition of glucose (1 mM) the topographic heights of BCNP increased (Fig. 5c, d), confirming the working mechanism shown in Scheme 1.

Conclusion

We have demonstrated a novel fluorescence carbon nanoparticle with high quantum yield integrated with smartphone for detection of glucose with the advantages of high sensitivity and selectivity. The probe was based on the combination of 4-CPBA, OPD and rhodamine B, and the green fluorescence of BCNP probe can be enhanced by increasing of glucose concentration. We further developed a cost-effective, portable POC device to detect the luminescence of BCNP probe and estimate glucose concentration. The method was used for selective glucose sensing at concentration range 32 μM to 2 mM with detection limit of 8 μM. Furthermore, the application of the assay for glucose measuring in serum samples was evaluated and the results were compared to standard method. The presence of two cis-diol units in glucose with the boronic acid groups on the BCNP surfaces created structurally rigid BCNP-glucose aggregates, resulting in a great boost in the fluorescent intensity. The smartphone based POC device functions through image analysis based methods to carry detection of glucose using RGB software analysis. In addition, the novel smartphone-based method meets the requirement of rapid and convenient to achieve glucose detection in serum sample and avoid complicated operations and expensive instruments. The current fluorescent strategies may be extended to apply the portable analysis in the biological, chemical and environmental fields and might hold great promise in nanomedicine. However, the irreversibility of fluorescence response is a challenge which limits the wider applicability of this method for online monitoring.

Compliance with ethical standards The author(s) declare that they have no competing interests.

References

1. Shaw JE, Sicree RA, Zimmet PZ (2010) Global estimates of the prevalence of diabetes for 2010 and 2030. Diabetes Res Clin Pract 87:4–14
2. Zou W-S, Ye C-H, Wang Y-Q, Li W-H, Huang X-H (2018) A hybrid ratiometric probe for glucose detection based on synchronous responses to fluorescence quenching and resonance light scattering enhancement of boronic acid functionalized carbon dots. Sensors Actuators B Chem 271:54–63
3. Sun K, Yang Y, Zhou H, Yin S, Qin W, Yu J, Chiu DT, Yuan Z, Zhang X, Wu C (2018) Ultrabright polymer-dot transducer enabled wireless glucose monitoring via a smartphone. ACS Nano 12:5176–5184
4. Murugaiyan SB, Ramasamy R, Gopal N, Kuzhandaivelu V (2014) Biosensors in clinical chemistry: an overview. Adv Biomed Res 3:67
5. Salimi A, Compton RG, Hallaj R (2004) Glucose biosensor prepared by glucose oxidase encapsulated sol-gel and carbon-nanotube-modified basal plane pyrolytic graphite electrode. Anal Biochem 333:49–56
6. Wang H-C, Zhou H, Chen B, Mendes PM, Fossey JS, James TD, Long Y-T (2013) A bis-boronic acid modified electrode for the sensitive and selective determination of glucose concentrations. Analyst 138:7146–7151
7. Salimi A, Roushani M (2005) Non-enzymatic glucose detection free of ascorbic acid interference using nickel powder and nafion sol–gel dispersed renewable carbon ceramic electrode. Electrochem Commun 7:879–887
8. Wang J, Thomas DF, Chen A (2008) Nonenzymatic electrochemical glucose sensor based on nanoporous PtPb networks. Anal Chem 80:997–1004
9. Na W, Liu H, Wang M, Su X (2017) A boronic acid based glucose assay based on the suppression of the inner filter effect of gold nanoparticles on the orange fluorescence of graphene oxide quantum dots. Microchim Acta 184:1463–1470
10. Zhou X, Gao X, Liu M, Wang C, Chu F (2017) A poly (5-indolylboronic acid) based molecular imprint doped with carbon dots for fluorometric determination of glucose. Microchim Acta 184:4175–4181
11. Wang W, Kong L, Zhu J, Tan L (2017) One-pot preparation of conductive composite containing boronic acid derivative for non-enzymatic glucose detection. J Colloid Interface Sci 498:1–8
12. Pham X-H, Shim S, Kim T-H, Hahm E, Kim H-M, Rho W-Y, Jeong DH, Lee Y-S, Jun B-H (2017) Glucose detection using 4-mercaptophenyl boronic acid-incorporated silver nanoparticles-embedded silica-coated graphene oxide as a SERS substrate. BioChip J 11:46–56
13. Nair PA, Sreenivasan K (2016) Non enzymatic colorimetric detection of glucose using cyanophenyl boronic acid included β-cyclodextrin stabilized gold nanoparticles. Anal Methods 8:2082–2087
14. Wang C, Li Y, Wei Y (2017) A sandwich boronate affinity sorbent assay for glucose detection facilitated by boronic acid-terminated fluorescent polymers. Sensors Actuators B Chem 247:595–601
15. Hamd-Ghadareh S, Salimi A, Fathi F, Bahrami S (2017) An amplified comparative fluorescence resonance energy transfer immunosensing of CA125 tumor marker and ovarian cancer cells using green and economic carbon dots for bio-applications in labeling, imaging and sensing. Biosens Bioelectron 96:308–316
16. Naaz S, Poddar S, Bayen SP, Mondal MK, Roy D, Mondal SK, Chowdhury P, Saha SK (2018) Tenfold enhancement of fluorescence quantum yield of water soluble silver nanoclusters for nano-molar level glucose sensing and precise determination of blood glucose level. Sensors Actuators B Chem 255:332–340
17. Pla-Tolós J, Moliner-Martínez Y, Molins-Legua C, Campins-Falco P (2018) Solid glucose biosensor integrated in a multi-well microplate coupled to a camera-based detector: application to the multiple analysis of human serum samples. Sensors Actuators B Chem 258:331–341
18. Wang L-J, Chang Y-C, Sun R, Li L (2017) A multichannel smartphone optical biosensor for high-throughput point-of-care diagnostics. Biosens Bioelectron 87:686–692
19. Zhang D, Liu Q (2016) Biosensors and bioelectronics on smartphone for portable biochemical detection. Biosens Bioelectron 75:273–284

20. Qu Z-B, Zhou X, Gu L, Lan R, Sun D, Yu D, Shi G (2013) Boronic acid functionalized graphene quantum dots as a fluorescent probe for selective and sensitive glucose determination in microdialysate. Chem Commun 49:9830–9832

21. Behzadi M, Noroozian E, Mirzaei M (2013) A novel coating based on carbon nanotubes/poly-ortho-phenylenediamine composite for headspace solid-phase microextraction of polycyclic aromatic hydrocarbons. Talanta 108:66–73

22. Cheng C, Zhang X, Wang Y, Sun L, Li C (2012) Phenylboronic acid-containing block copolymers: synthesis, self-assembly, and application for intracellular delivery of proteins. New J Chem 36:1413–1421

23. Jiang Z, Dong B, Chen B, Wang J, Xu L, Zhang S, Song H (2013) Multifunctional au@ mSiO2/rhodamine B isothiocyanate nano-composites: cell imaging, photocontrolled drug release, and photothermal therapy for cancer cells. Small 9:604–612

24. Cordes DB, Gamsey S, Singaram B (2006) Fluorescent quantum dots with boronic acid substituted viologens to sense glucose in aqueous solution. Angew Chem Int Ed 45:3829–3832

25. Lan M, Zhang J, Chui Y-S, Wang H, Yang Q, Zhu X, Wei H, Liu W, Ge J, Wang P (2015) A recyclable carbon nanoparticle-based fluorescent probe for highly selective and sensitive detection of mercapto biomolecules. J Mater Chem B 3:127–134

26. Diac A, Focsan M, Socaci C, Gabudean A-M, Farcau C, Maniu D, Vasile E, Terec A, Veca LM, Astilean S (2015) Covalent conjugation of carbon dots with rhodamine B and assessment of their photophysical properties. RSC Adv 5:77662–77669

27. Heller A, Feldman B (2008) Electrochemical glucose sensors and their applications in diabetes management. Chem Rev 108:2482–2505

28. Wu W, Zhou T, Berliner A, Banerjee P, Zhou S (2010) Glucose-mediated assembly of Phenylboronic acid modified CdTe/ZnTe/ZnS quantum dots for intracellular glucose probing. Angew Chem Int Ed 49:6554–6558

29. Wu W, Zhou T, Shen J, Zhou S (2009) Optical detection of glucose by CdS quantum dots immobilized in smart microgels. Chem Commun 14(29):4390–4392

30. Wang D, Liu T, Yin J, Liu S (2011) Stimuli-responsive fluorescent poly (N-isopropylacrylamide) microgels labeled with phenylboronic acid moieties as multifunctional ratiometric probes for glucose and temperatures. Macromolecules 44:2282–2290

31. Wang L-L, Qiao J, Liu H-H, Hao J, Qi L, Zhou X-P, Li D, Nie Z-X, Mao L-Q (2014) Ratiometric fluorescent probe based on gold nanoclusters and alizarin red-boronic acid for monitoring glucose in brain microdialysate. Anal Chem 86:9758–9764

32. Basiruddin S, Swain SK (2016) Phenylboronic acid functionalized reduced graphene oxide based fluorescence nano sensor for glucose sensing. Mater Sci Eng C 58:103–109

33. Chibac AL, Melinte V, Buruiana T, Buruiana EC (2017) Fluorescent polymeric sensors containing boronic acid derivatives for sugars and dopamine detection. Sensing characteristics enhancement by au NPs. Sensors Actuators B Chem 253:987–998

34. Dong J, Li X, Zhang K, Di Yuan Y, Wang Y, Zhai L, Liu G, Yuan D, Jiang J, Zhao D (2018) Confinement of aggregation-induced emission molecular rotors in ultrathin two-dimensional porous organic nanosheets for enhanced molecular recognition. J Am Chem Soc 140:4035–4046

35. Mei J, Hong Y, Lam JW, Qin A, Tang Y, Tang BZ (2014) Aggregation-induced emission: the whole is more brilliant than the parts. Adv Mater 26:5429–5479